JOURNAL OF MECHANICS OF CONTINUA AND MATHEMATICAL SCIENCES
www.journalimcms.org

ISSN (Online) : 2454 -7190 Vol.-16, No.-5, May (2021) pp 36-48 ISSN (Print) 0973-8975

INFLUENCE OF TEMPERATURE AND DRAWING SPEED ON THE FORMING OF ALUMINUM ALLOY 1100 VIA WARMING HYDROFORMING PROCESS

Mohammed Mishri Gatea[1], Hani Aziz Ameen[2], Haidar Akram Alsabti[3]

[1,2,3]Middle Technical University- Technical Engineering College, Baghdad

[1]eng.moh251@yahoo.com, [2]prof.dr.hani@gmail.com, [3]drhaidarakram2020@gmail.com

https://doi.org/10.26782/jmcms.2021.05.00004

(Received: February 14, 2021; Accepted: April 27, 2021)

Abstract

The limiting use of the alloys of aluminum is since the formability is low at room temperature. To plan and grow more parts made of aluminum, new forming systems, for example, warm framing hydroforming and warming hydroforming processes have been explored to solve the low formability. The effect of temperature on the mechanical properties of aluminum 1100 sheet alloy is investigated at different temperature levels and strain rates using the test of uni-axial tensile. A warming forming tool for sheet metal is designed and manufactured. Four temperatures levels were used in this experiments (25℃, 100℃, 200℃, and 300℃). The drawing speeds that were used in these experiments were (3, 6, and 9 mm/min). Before designing the warming hydro-punch system, the analysis of this system is done in ANSYS software to choose the optimum die radius and then the results of the experiments are simulated. The results of experiments showed that the appropriate hydroforming temperature and drawing speed of 1100 aluminum alloy are 300℃ and 3mm/min respectively. The FE simulation of strain distribution matched reasonably well with the experimental results.

Keywords: Deep drawing process, 1100 aluminum alloy, Formability, hydro-punch, ANSYS, warming hydroforming process

I. Introduction

The pressure of the fluid is utilized in the hydroforming process to get the required shape of the product as shown in Figure 1. The pressure of the fluid causes uniform straining of material which leads to a regular rising in yield strength in the utilized material and this leads to lower thinning (Hein, & Vollertsen, 1999). It is additionally alluded to as punchless hydroforming, simply hydroforming or high-pressure sheet forming (Modi & Kumar, 2013). The warm Hydroforming technique has the advantages of both warm forming and Hydroforming (Billur, 2008). The low formability of aluminum and magnesium alloys at room temperatures, particularly in conventional metal stamping processes, has limited their wide application (Yuan, et al., 2006). Is notable that formability of the lightweight materials such as aluminum alloys is incremented at raised temperature levels (Li & Ghosh, 2003) (Naka, et al., 2001). Warming hydroforming and warm stamping are two such processes that have obtained considerable interest recently (Shah, et al., 2011). Warm hydroforming acts

decreasing the required closing force in hydroforming and decreasing the forming temperature in warm forming in warm forming (Koç, 2008). In general, this process presents improved formability, reduced processing, part consolidation, mass reduction, and the possibility for overall cost reduction (Koç, et al., 2011). In this study, our objectives were to: (1) practically comprehend and evaluate the influences of the parameters of the process, like temperature and drawing speed, on the forming product via the height of the dome and thickness distribution with complex geometries and, (2) built a finite element model (FEM) through ANSYS software to choose the optimal die radius for hydroforming test and simulation the practical experiment and comparison the results.

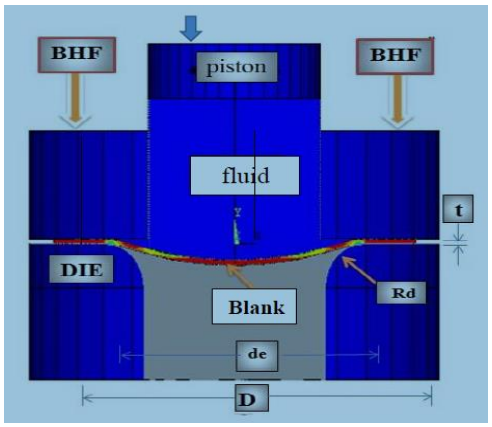

Figure 1. Items of the hydroforming process

II. Experimental Part

The chemical compositions were determined using Spectro max X instrument, results of which are, as shown in Table 1.

Table 1: Chemical composition of aluminum alloy 1100 sheet.

Sample	Si%	Fe%	Cu%	Mn%	Mg%	Cr%	Ni%	Zn%	Ti%	Sn%	V%	Pb%	Al%
Al	0.0524	0.255	0.0011	0.0016	0.0008	0.003	<0.00i	0.013	0.0163	<0.0005	0.0066	<0.0005	Bal

To study the material behavior of aluminum alloy 1100 under different process conditions (temperature and strain rate), the results of the tensile experiments at different deformation temperatures and strain rate which performed by (Meriç, et al.,1997) were depended as shown in Table 2.

Table 2: Mechanical properties of aluminum alloy 1100 at different temperature and strain rates (Koç, 2008).

Temperature [°C]	Strain rate $[10^{-4}]$ $[s^{-1}]$	Yield strength [MPa]	Tensile Strength [MPa]	Elongation [%]
20	2	119	155	22.5
20	4	199	150	20
20	20	125	152	20
100	2	117	137	22.5
100	4	11	130	22.5
100	20	121	135	20
200	2	84	94	20
200	4	85	93	20.7
200	20	86	88	20
300	2	24	29	30
300	4	24	30	26.5
300	20	29	30	32.5

The tool of warm hydroforming metal sheet placed on the Compression test apparatus is characterized by max load (200KN) and ram velocity (3, 6, and 9 mm/min). To study the strain distribution on the final product, grid pattern squares of (4×4) mm are printed on all specimens. The first step is filling the cylinder of the sheet hydroforming tool (SHF) with oil. Then, a circular blank has been put between the blank holder and the die. The diameter of the blank is 80mm and the thickness is 1mm. The optimal die radius is 8mm was chosen using the finite element method via Ansys software. The die radiuses that are used in the simulation are (2, 4, 6, 8, and 10) mm. The results show that the optimal distribution of Von-Misses stresses when the die radius is 8mm. Figure 2. Show Von-Misses stress distribution. After this, blank holder force (BHF) has been forced by using eight screw bolts and a torque arm to avoid wrinkling and tearing. In the second step, the die and die house and the sheet and blank holder are warmed to the necessary temperature. For the heating system, cartridge heaters, temperature controllers and thermocouples are used. In the last step moving the piston through the Compression test apparatus, the continuous progress of the piston leads to move the wave's load of the oil pressure which causes deforming of the blank. This operation is repeated for each temperature and drawing speed. Figure3. Show Compression Test apparatus with the tools of warming hydroforming process. Figure 4. Show the experimental rig of the warming hydroforming process.

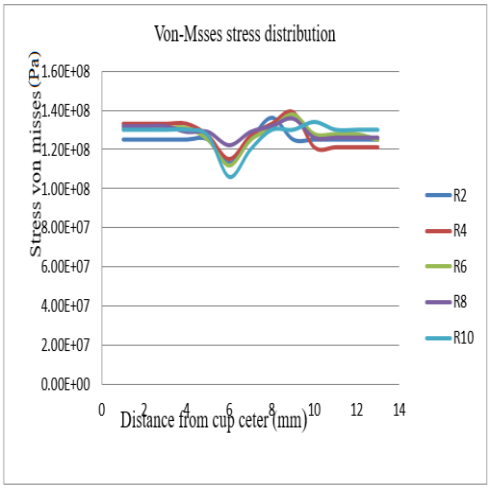

Figure 2. Von-Misses stress distribution

Figure 3. Compression Test apparatus with the tool of hydroforming

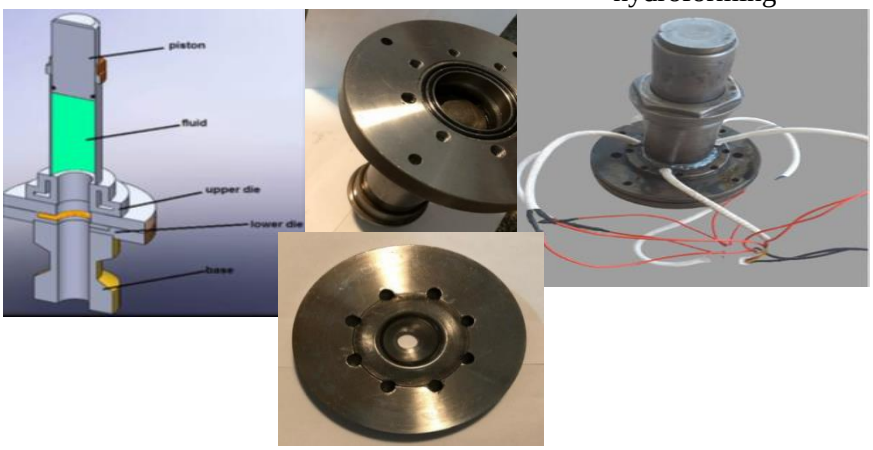

Figure 4. Tool of the warming hydroforming process

III. Simulation of hydro Deep Drawing Process

In this examination, a universally useful linear and nonlinear finite element method investigation program, ANSYS 2019 R1 is utilized to develop the finite element model. Command files APDL-ANSYS code is created to simulate the hydro deep drawing process (Nakasone and Yoshimoto, 2006), which is programmed the general constitutive equation of stress-strain relations with effect the temperature is based on the assumption that the total strain is decomposable into a strain component due to elastic deformation, temperature-dependent material properties, thermal strain and plastic strain (Modi, & Ravi Kumar, 2013).

Beginning from the presumption that the total strain is severable into a:

$$d\underline{\varepsilon} = d\underline{\varepsilon}^{(e)} + d\underline{\varepsilon}^{(dm)} + d\underline{\varepsilon}^{(T)} + d\underline{\varepsilon}^{(p)} \quad (1)$$

Now, from Hook's law, $d\underline{\sigma} = [D]\, d\underline{\varepsilon}^{(e)}$, where [D] is an elasticity matrix, $d\underline{\varepsilon}^{(T)} = \underline{\alpha}.dT$, the flow rule is $d\underline{\varepsilon}^{(p)} = d\lambda\,.\,\underline{a}$,

Where $\underline{a}$ $=\partial\underline{\sigma}$, where $\underline{a}$ $=\partial F/\partial\underline{\sigma}$, and it can be proved that $d\underline{\varepsilon}^{(dm)} = (\partial[D]^{-1}/\partial T)\,\underline{\sigma}dT$.

Substitute all these relations into Eq.(1), it can be deduced that:

$$d\underline{\sigma} = [D]d\underline{\varepsilon} - [D]\left(\underline{\alpha}dT + \frac{\partial[D]^{-1}}{\partial T}\underline{\sigma}dT\right) - [D]d\lambda\underline{\alpha} \quad (2)$$

The two-dimensional model is built in the preprocessor program via Ansys, because of the geometry and conditions of loading of the actual framework which can be sensibly approximated using the model of an axisymmetric, two dimensions are used to model, the computational expense of an entire three-dimensional model is evaded.
For the processes of deep drawing simulation, finite element models (FEM) through Ansys software are utilized, that the implicit approach "Newton-Raphson" was used to solve the problem of nonlinearity. In this method, the steps of stroke on the apparatus were characterized explicitly over some time. Many solutions are done for each step, (sub-steps or time steps) were worked to make the displacement bit by bit (Ameen, 2010). Several iterations of equilibrium are evaluated within each sub-step, to get a convergence solution. The Newton-Raphson method calculated the load vector of out-of-balance before each solution that was the divergence between the restoring forces and the applied loads. A linear solution is done by the Ansys program by the out-of-balance loads and investigate for the converge criteria. If the criteria converge is not fulfilled, the out-of-balance load vector was re-calculated, the stiffness matrix is updating, and a new solution is gotten. The procedure of iteration is continued till the convergence is exists. The Solid182 two-dimension four-node structural solid element was utilized for blank with axis-symmetric key option (ET, 1,182, KEYOPT,1,3,1) (ANSYS 19.0 R1 User guide, 2019). The die and punch set was modeled as rigid bodies (Al-Saadi, et al., 2011). The 2-D 4-node contained fluid element Fluid79 was used for hydraulic oil. A pilot node is utilized to represent the moving of the punch and holding force. An automatic contact procedure in ANSYS 2019 R1 was utilized to model the complex interaction between the blank and tooling.
Due to the axisymmetric in the blank geometry, constraints and boundary conditions, the axisymmetric part of the model is required to be studied. The geometry of the hydro deep drawing process utilized in the simulating is shown in Figure 1.

IV. Results and Discussion

IV.i. Hydro-Punch Load

Figure 5. shows the deformed blanks which were hydroformed at room temperature (25°C), 100 °C, 200 °C, and 300 °C and drawing speeds 3, 6, and 9 mm/min.

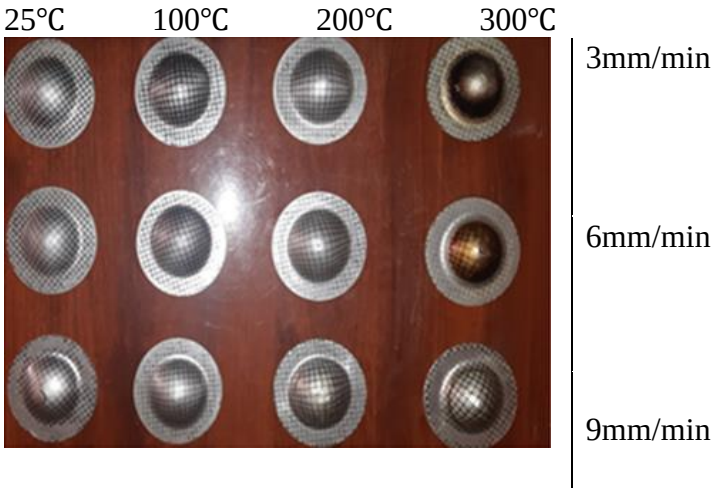

Figure 5. Hemispherical cups

The relations between the load and displacement of hydro punch at these conditions are found as shown in Figure 6.a, b, c. The results to some extent are convergent where the displacement is increased when the drawing speed is increased. On the other hand, the effect of temperature on the loads required to the deforming was obvious particularly when the temperature is increased from room temperature to 200℃ and 300. In the 300℃, the effect of temperature on displacement and deforming load was very obvious at all drawing speeds especially at 3mm/min as shown in Figure 6.d. Figure 7. Show the influence of the temperature on displacement and deforming load at drawing speed 3mm/min.

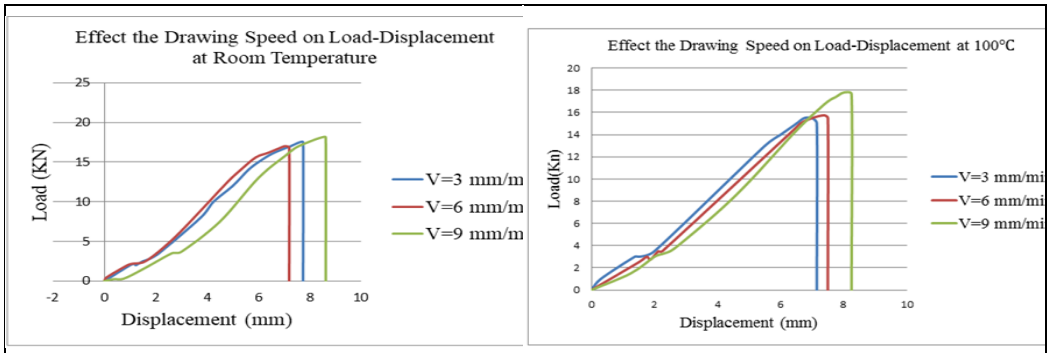

a b

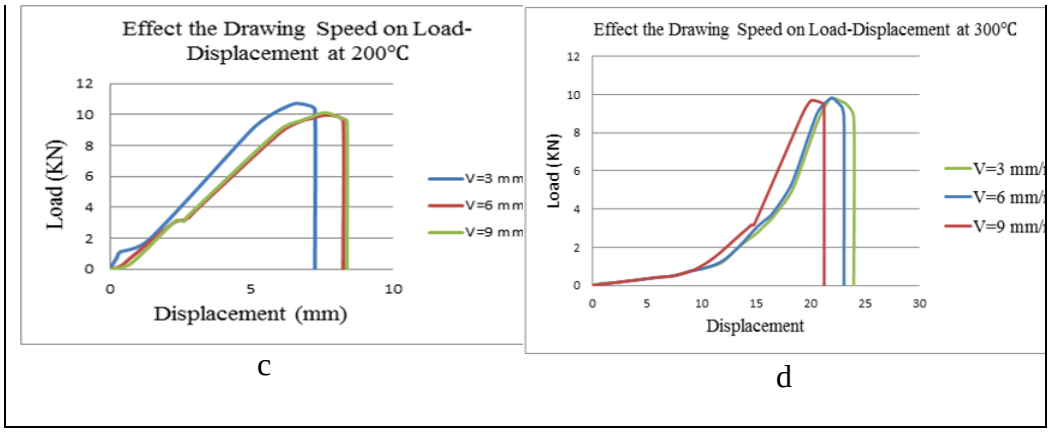

Figure 6. Effect the temperature and drawing speed of hydro- punch and deformation load of aluminum alloy 1100

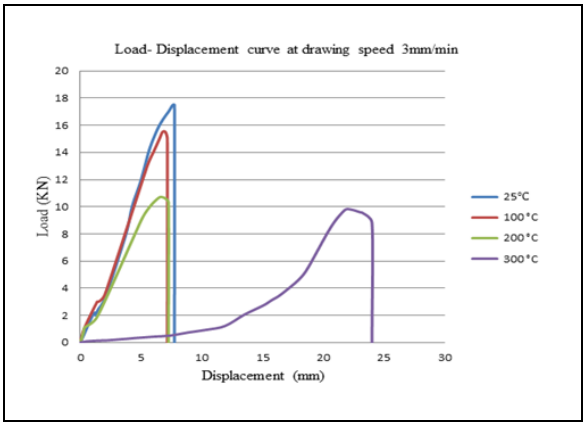

Figure 7. Effect the temperature on the displacement of hydro-punch and deformation load of aluminum alloy 1100 at drawing speed 3mm/min

IV.ii. Strain distribution

Figure 8.a, b, c and d shows the effect of temperature on the strain distribution at different drawing speeds. In any case of forming, the strain distribution change at all the regions from edge to the center of the cup. The first zone starts from the edge of the blank to begin the radius of the die which represents the region that contact with the blank holder, the strains in this zone are very small due to the action of blank holder force and the friction between the blank holder and the blank which restrains the flowing of the metal into the inside of the die. The second zone is the radius of the die (8 mm) which the strains are increased compared to the first zone. The strain in this region is small due to the friction between the blank and surface of the die and this region consider zone of stress concentration. In the last region, the flowing of metal into the die is free and the stresses in this zone are tensile stresses, thus the strains are increased. In the next zone, the strain begins decreased then increased until

the dome height is reached to the maximum value or the dome is tearing before this. The effect of temperature was obvious particularly at 300℃ and 3mm/min which more uniform from the other temperature level and drawing speeds.

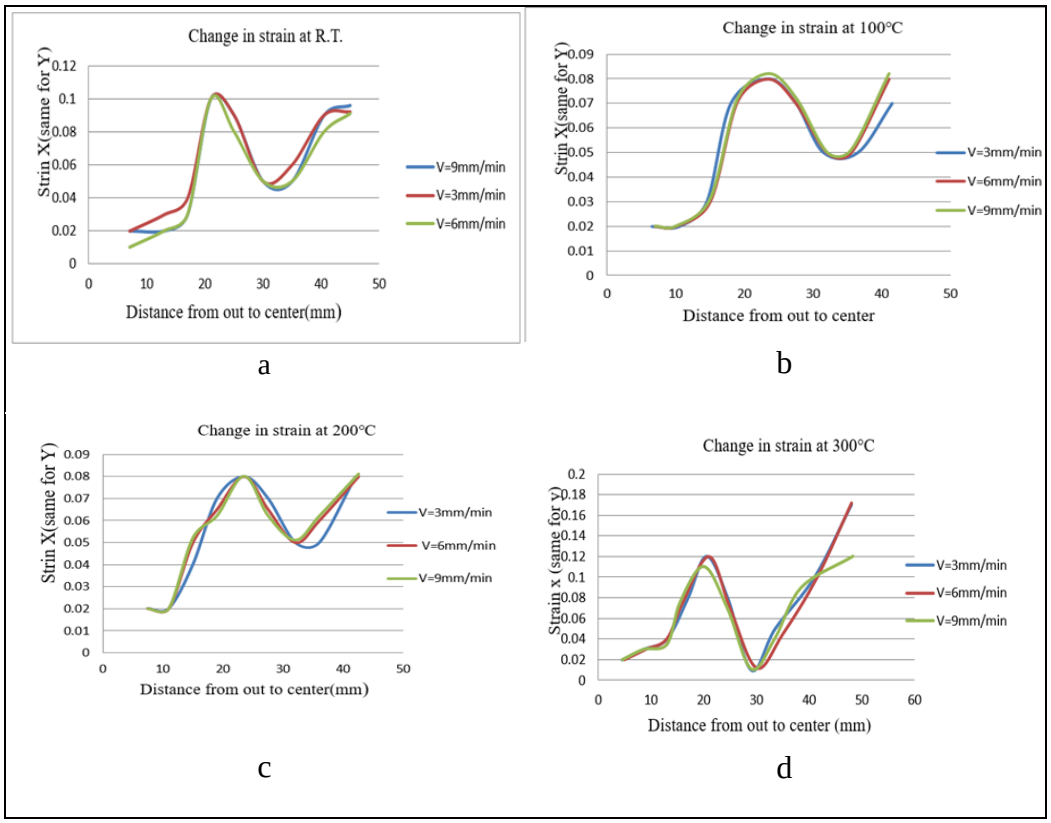

Figure 8. Effect the temperature and drawing speed on strain distribution

Figure 9.a, b, c illustrated the comparison results of strain distribution for die profile (8mm) between ANSYS results and experimental at 300 ℃ and drawing speed (3, 6, and 9) mm/min. Good agreement is evident.

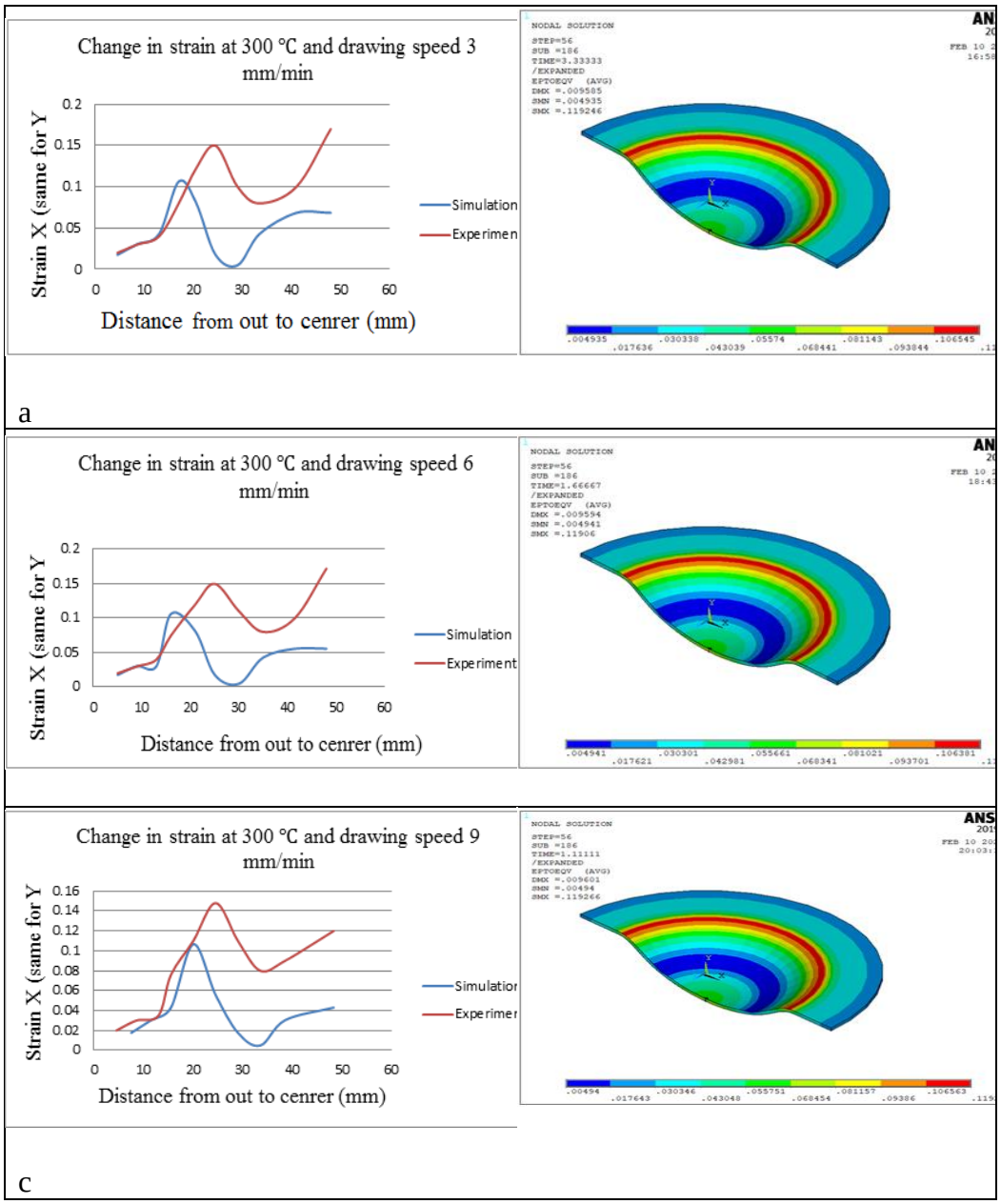

Figure 9. a, b, c: Comparison results of strain distribution for die profile (8mm) between ANSYS results and experimental

IV.iii. Wall Thickness Distribution

The relation between thickness wall distributions of the final product from the cup center to the outside edge is found. The strain distribution which is indicated through the grid square resembles the wall thickness distribution. When the strain is increased, the wall thickness is decreased. It is obvious that the thickness is changing

under the hydraulic base of the punch due to no friction which prevents the deformation. In the next region, thinning will happen, since an increase in stretching exercised used the high tensile stress in this zone. In the zone of the die surface, the change in wall thickness decreases due to the friction between the blank and die surface. Less change in wall thickness is occurring in the zone of the blank holder, due to the action of the friction and blank holder force which prevent or restrain the deformation. Thicken will occur at the outside edge, due to the hoop stress (circumference). Figure 10.a, b, c, and d showed the influence of temperature and drawing speed on the wall thickness distribution.

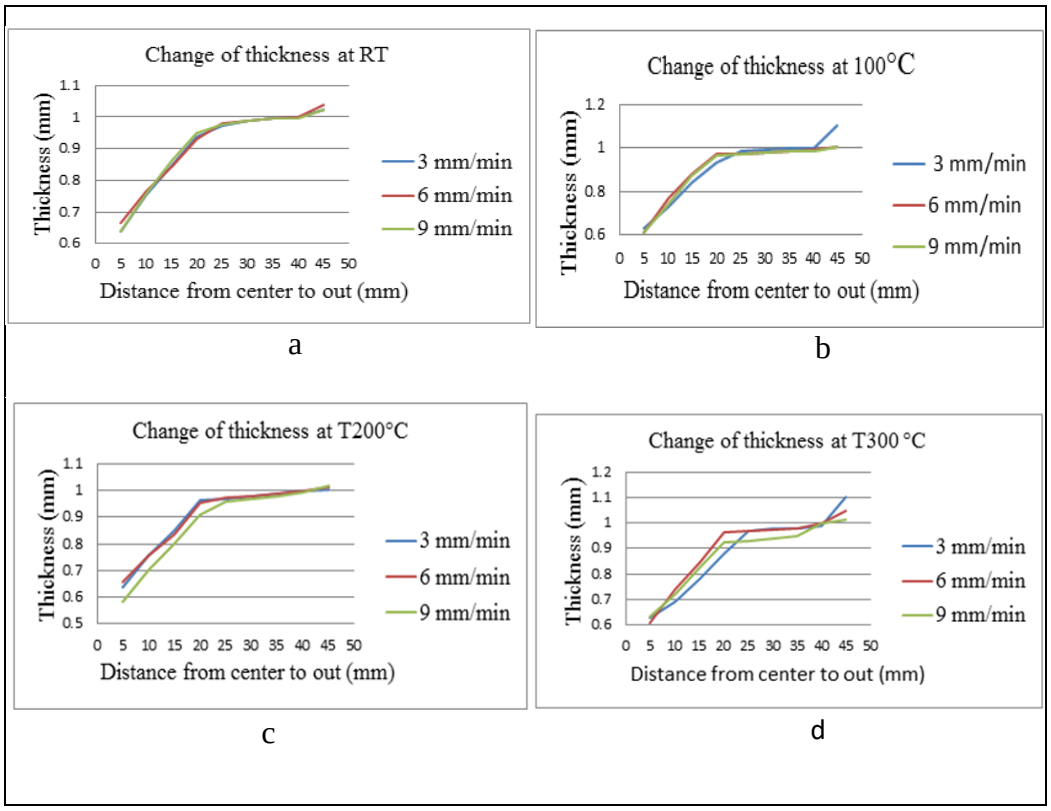

Figure 10. a, b, c, d: Effect of temperature and drawing speed on the wall thickness distribution

IV.iv. Dome height

The increase in the dome height was evident in the experiments carried out at 300℃ and drawing speeds (3, 6, 9 mm/min) as shown in Figure 11. The dome of the cup was spherical in these experiments, unlike other experiments which resemble a cone as shown in Figure 5. This explains that the displacement of hydro punch is much greater than the increase of dome height when the experiments are achieved at 300℃

as shown in Figure 7. Table 3. Show the effect of temperature and drawing speed on the dome height.

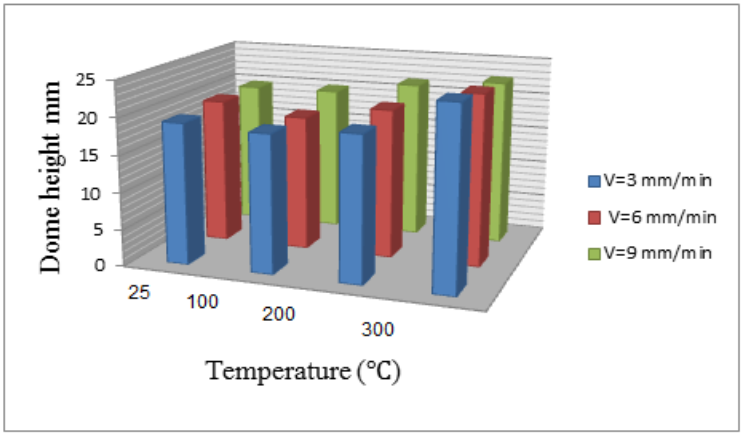

Figure 11. Effects of the temperature and drawing speed to the dome height

Table3: Effect of temperature and drawing speed on the dome height.

Test number	Dome height (mm)	Drawing speed (mm/min)	Temperature (°C)
1	19.18	3	25
2	19.77	6	25
3	19.72	9	25
4	18.71	3	100
5	18.37	6	100
6	19.86	9	100
7	19.61	3	200
8	20.26	6	200
9	21.50	9	200
10	24.38	3	300
11	23.23	6	300
12	22.54	9	300

V. Conclusions

In this study, the formability of the aluminum 1100 sheet was investigated using both tensile test and hydroforming experiment at temperature levels (25℃,100℃, 200℃, 300℃) and drawing speed (3, 6, 9mm/min). A special tool for sheet warming hydroforming was designed and manufacturing. The tensile test at elevated temperatures was utilized to study the forming of the typical aluminum sheet at high temperatures. It was shown that the results of the hydroforming experiment are in good agreement with the results of the tensile test concerning enhancing the formability after 300℃ since the thermally activated dislocation lines. The results of the experiment showed that the maximum thinning for all temperature levels has occurred at the region near the center of the cup. The formability is enhanced at 300℃ with a decrease in the drawing speed. Thus the optimal temperature and drawing speed for warming hydroforming process of aluminum alloy 1100 is 300℃ and 3mm/min respectively. The forming load is decreased when the temperature is reached 200℃. The results of the finite element method showed that the optimal die radius for the hydroforming aluminum alloy 1100 is 8mm.

VI. Acknowledgements

We would like to express our thanks to the staff of the Institute of Technology/Baghdad in Middle Technical University for their help.

Conflict of Interest:

There is no conflict of interest regarding this article

References

I. ANSYS 19.0 R1 User guide, 2019.

II. Agarwal A., Seretse O.M., Pumwa J. : 'FINITE ELEMENT AND TAGUCHI RESPONSE ANALYSIS OF THE APPLICATION OF GRAPHITE ALUMINIUM MMC IN AUTOMOTIVE LEAF SPRING.' *J. Mech. Cont.& Math. Sci.*, Vol.-15, No.-7, July (2020) pp 168-179. DOI : 10.26782/jmcms.2020.07.00013

III. Billur, E. (2008). Warm Hydroforming Characteristics of Stainless Steel Sheet Metals.

IV. Cevdet Meriç, Enver Atik, Erdoğan Özkaya (1997). Investigation of Deformation Temperatures and Strain Rate Effects' on the Mechanical Properties of Al 99.0. Pamukkale Univ Muh Bilim Derg. 3(1): 293-298.

V. Hein, P., & Vollertsen, F. (1999). Hydroforming of sheet metal pairs. Journal of Materials Processing Technology, 87(1-3), 154-164.

VI. Hani Aziz Ameen (2010). " Study the stresses in deep drawing process using conical die", Journal of Kerbala University,Vol.8, No.1,Sientific,(in Arabic) .

VII. Koç, M. (Ed.). (2008). Hydroforming for advanced manufacturing. Elsevier.

VIII. Koç, M., Agcayazi, A., & Carsley, J. (2011). An experimental study on robustness and process capability of the warm hydroforming process. *Journal of manufacturing science and engineering*, *133*(2).

IX. Li, D., & Ghosh, A. (2003). Tensile deformation behavior of aluminum alloys at warm forming temperatures. *Materials Science and Engineering: A*, *352*(1-2), 279-286.

X. Modi, B., & Ravi Kumar, D. (2013). Effect of friction and lubrication on formability of AA5182 alloy in hydroforming of square cups. In Materials Science Forum (Vol. 762, pp. 621-626). Trans Tech Publications Ltd.

XI. Moneer H. Al-Saadi, Hani Aziz Ameen & Rawa Hamed M. Al-Kalali (2011). "Influence of Metal Type on the Deep Drawing Force by Experimental and Finite Element Method", Engineering and Technology Journal, Vol.29, No.13.

XII. Modi, B., & Ravi Kumar, D. (2013). Effect of friction and lubrication on formability of AA5182 alloy in hydroforming of square cups. In Materials Science Forum (Vol. 762, pp. 621-626). Trans Tech Publications Ltd.

XIII. Naka, T., Torikai, G., Hino, R., & Yoshida, F. (2001). The effects of temperature and forming speed on the forming limit diagram for type 5083 aluminum–magnesium alloy sheet. *Journal of Materials Processing Technology*, *113*(1-3), 648-653.

XIV. Nakasone Y. and Yoshimoto S. (2006). "Engineering Analysis with ANSYS Software", Department of Mechanical Engineering, Tokyo University of Science.

XV. Shah, M., Billur, E., Sartkulvanich, P., Carsley, J., & Altan, T. (2011, August). Cold and Warm Hydroforming of AA754-O Sheet: FE Simulations and Experiments. In *AIP Conference Proceedings* (Vol. 1383, No. 1, pp. 690-697). American Institute of Physics.

XVI. Umair Aftab, Muhammad Mujtaba Shaikh, Muhammad Ziauddin Umer. : 'A NEW AND RELIABLE STATISTICAL APPROACH WITH EFFECTIVE PROFILING OF HARDNESS PRESERVING SAMPLES IN TIG-WELDING, THERMAL TREATMENT AND AGE-HARDENING OF ALUMINUM ALLOY 6061'. *J. Mech. Cont.& Math. Sci.*, Vol.-15, No.-11, November (2020) pp 108-118. DOI : 10.26782/jmcms.2020.11.00010

XVII. Yuan, S., Qi, J., & He, Z. (2006). An experimental investigation into the formability of hydroforming 5A02 Al-tubes at elevated temperature. *Journal of Materials Processing Technology*, *177*(1-3), 680-683.